



Supporting Online Material for  
**Molecular Identity of Dendritic Voltage-Gated Sodium Channels**

Andrea Lorincz\* and Zoltan Nusser\*

\*To whom correspondence should be addressed.  
E-mail: nusser@koki.hu (Z.N.); lorincz@koki.hu (A.L.)

Published 14 May 2010, *Science* **328**, 906 (2010)  
DOI: 10.1126/science.1187958

**This PDF file includes:**

Materials and Methods  
Figs. S1 to S5

## Supporting Online Material

### Materials and Methods

*Fluorescence immunohistochemistry.* Adult male Wistar rats were deeply anesthetized with ketamine before transcardial perfusion with ice-cold fixative containing 1-2% paraformaldehyde in 0.1M Na-phosphate (PB, pH = 7.3) or in Na-acetate buffer (pH = 6; Berod et al., 1981, J Histochem Cytochem 29 : 844-850) for 10-25 minutes. 60  $\mu$ m thick coronal sections were cut from the forebrain with a Vibratome and were washed in 0.1M PB. Sections were then blocked in 10% normal goat serum (NGS) made up in Tris-buffered saline (TBS, pH = 7.4), followed by incubations in primary antibodies diluted in TBS containing 2% NGS and 0.1% Triton X-100. Following several washes, the following secondary antibodies were used to visualize the immunoreactions: Alexa488-conjugated goat anti-rabbit and anti-mouse (1:500) and Cy3-conjugated goat anti-rabbit, anti-mouse and donkey anti-guinea pig (1:500). Sections were then mounted on glass slides in Vectashield. Specificity of the immunoreactions for Nav1.2 and Nav1.6 subunits was tested in double labeling experiments using two antibodies raised against different, non-overlapping epitopes.

*Antibodies.* The following antibodies were used: mouse anti-Nav1.1 (diluted in 1:250), rabbit anti-Nav1.2 (1:500), mouse anti-Nav1.2 (1:500), rabbit anti-Nav1.6 (1:100), mouse anti-Nav1.6 (1:500), rabbit anti-pan-Nav (1:500), mouse anti-pan-Nav (1:1000), mouse anti-Ankyrin-G (1:500), guinea pig anti-VGluT1 (1:1000), rabbit anti-Kv4.2 (1:500), rabbit anti-Kv3.1b (1:500), mouse anti-Kv2.1 (1:250) and guinea pig anti-GABA<sub>A</sub> receptor  $\alpha$ 2 (1:1000; gift from Prof. J-M. Fritschy).

*SDS-digested freeze-fracture replica-labeling (SDS-FRL).* Adult male Wistar rats were deeply anesthetized and were transcardially perfused with ice-cold fixative containing 2% or 4% (only for the Ankyrin-G labeling) paraformaldehyde in 0.1M PB for 15 minutes. 80  $\mu$ m thick sections were cut from the forebrain and cryoprotected in 30% glycerol. Small blocks from the hippocampal CA1 area were sandwiched between copper carriers and were frozen with a high pressure freezing machine. Carriers were inserted into a double replica table and were fractured in a freeze-fracture machine.

Fractured faces were coated on a rotating table by carbon (5 nm) with an electron beam gun positioned at 90°, then shadowed with platinum (2 nm) at 60° unidirectionally (rotation stopped), followed by a final carbon coating (20 nm). Tissue debris was digested from the replicas with gentle stirring in a TBS solution containing 2.5% SDS and 20% sucrose (pH = 8.3) at 80°C overnight. The replicas were washed in TBS containing 0.05% bovine serum albumin (BSA) and blocked with 5% BSA in TBS for one hour. This was followed by an overnight incubation in the blocking solution containing the following primary antibodies: rabbit anti-Nav1.6 (1:500); mouse anti-pan-Neurofascin (1:300); mouse anti-Ankyrin-G (1:500); rabbit anti-GABA<sub>A</sub>β3 (1:500; gift from Prof. W. Sieghart), rabbit anti-Neurologin-2 (1:500). Replicas were then incubated in the blocking solution containing the following secondary antibodies: goat anti-rabbit and goat anti-mouse IgGs coupled to 10 or 15 nm gold particles (1:50). Replicas were rinsed in TBS and distilled water, before they were picked up on copper parallel bar grids. Replicas were then examined with an electron microscope. For stereoscopic images, regions of interest were examined and digital images were taken without and with 8 degree tilt of the goniometer (see fig. S5).

*Quantitative analysis of immunogold labeling for the Nav1.6 subunit.* Only large, complete replicas with clearly distinguishable alveus, strata oriens (SO), pyramidale (SP), radiatum (SR) and lacunosum-moleculare were subjected to quantitative analysis (n = 5 rats). Immunoreactions with a 10 nm gold-conjugated IgGs gave higher density of labeling therefore only those reactions were used for quantification. Images of identified profiles were taken with a Cantega G2 camera at 10000-12000x magnification in each layer. Nodes of Ranvier were sampled in the alveus. P-faces of Ranvier nodes were often seen at steep angle and were therefore tilted to maximize the two-dimensional view of the labeled membrane area. Images of AISs of CA1 PCs were taken in the SP and SO. Electron micrographs of proximal and distal dendrites were taken in the SR at 25-50 μm and 100-150 μm distances from the SP, respectively. Dendritic P-faces were identified as PC dendrites if at least one

spine protruded from it or if it contained partially fractured or cross-fractured spines. To avoid bias in the density calculations caused by the convex curvature of surfaces, only the central, approximately flat membrane areas were included in the measurements (steep, peripheral sides of P-faces were excluded from the analysis). Gold particle counting and area measurements were performed with the iTEM software. Nonspecific labeling for the Nav1.6 subunit was determined by counting immunogold particles on the E-face of PC somata and dendrites. Gold particle densities are represented as mean  $\pm$  SD between animals.

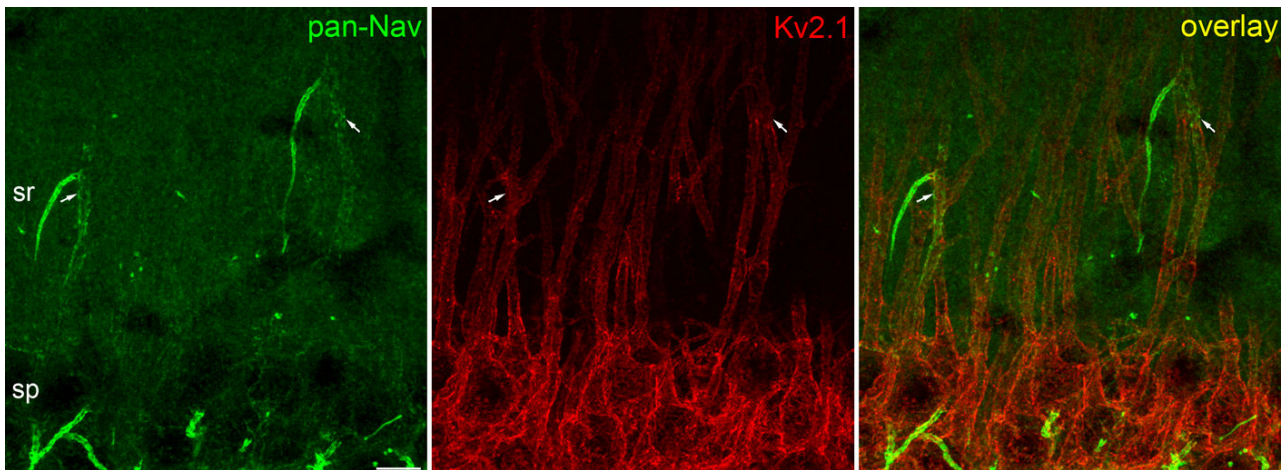


**Fig. S1.** Immunofluorescence localization of voltage-gated sodium channels in dendrites.

Immunofluorescent reaction reveals two strongly pan-Nav labeled (green) AISs in the stratum radiatum emerging from pyramidal cell apical dendrites. The apical dendrites (arrows) at the origin of the AISs contain detectable density of pan-Nav immunolabeling. The somato-dendritic plasma membranes of PCs were visualized by immunolabeling for the Kv2.1 subunit (red). sr: stratum radiatum, sp: stratum pyramidale; Scale bar: 10  $\mu$ m.

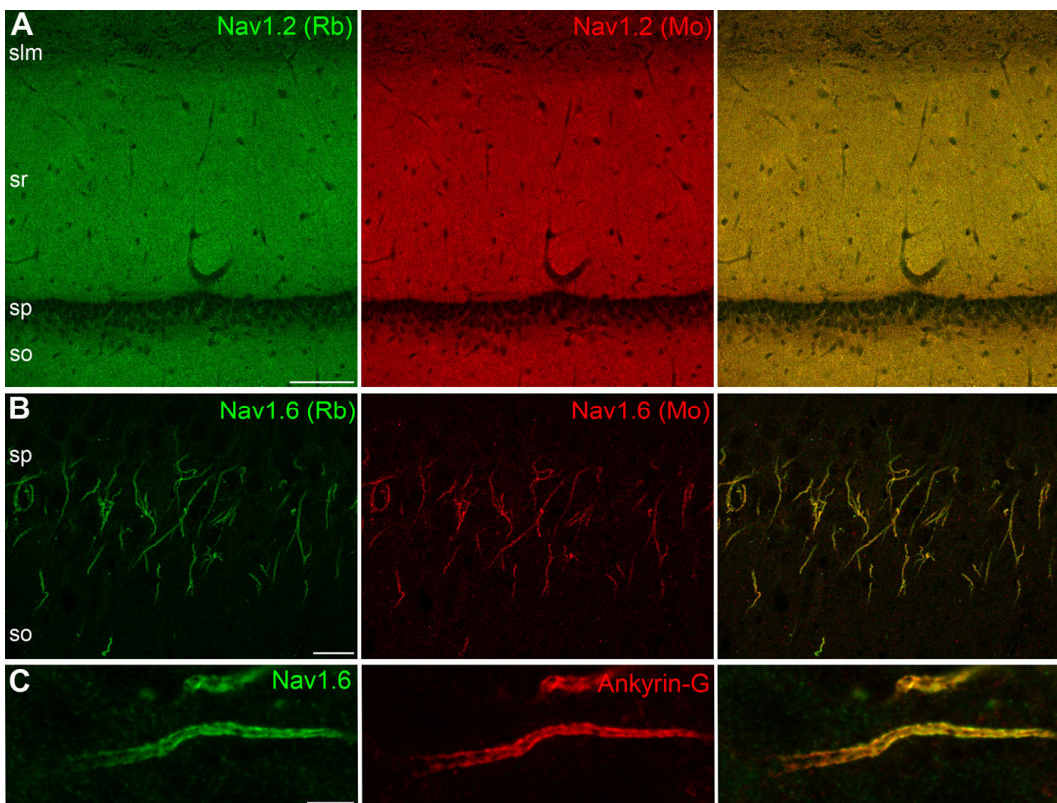


**Fig. S2.** Specificity tests of the Nav1.2 and Nav1.6 subunit immunoreactions using antibodies raised against different epitopes. **(A)** Double immunofluorescence reaction using a rabbit anti-Nav1.2 antibody, recognizing the intracellular loop between domains I and II (Nav1.2 (Rb), green) and a mouse anti-Nav1.2 antibody, recognizing the intracellular C-terminus (Nav1.2 (Mo), red). The identical immunolabeling of the CA1 area indicates that all labeling is due to the specific antibody-Nav1.2 subunit interaction. **(B)** Double immunofluorescence reaction using a rabbit anti-Nav1.6 antibody, recognizing the intracellular loop between domains II and III (Nav1.6 (Rb), green) and a mouse anti-Nav1.6 antibody recognizing the intracellular loop between domains I and II (Nav1.6 (Mo), red). Both antibodies strongly labeled all AISs in strata pyramidale and oriens. **(C)** Double immunofluorescence reaction demonstrating the colocalization of the Nav1.6 subunit (green) and Ankyrin-G (red) in the AIS of a PC in the stratum pyramidale. The panel showing Nav1.6 immunoreactivity is also shown in Fig. 3G. slm: stratum lacunosum-moleculare, sr: stratum radiatum, sp: stratum pyramidale, so: stratum oriens; Scale bars: **A**, 100  $\mu$ m; **B**, 20  $\mu$ m; **C**, 5  $\mu$ m.

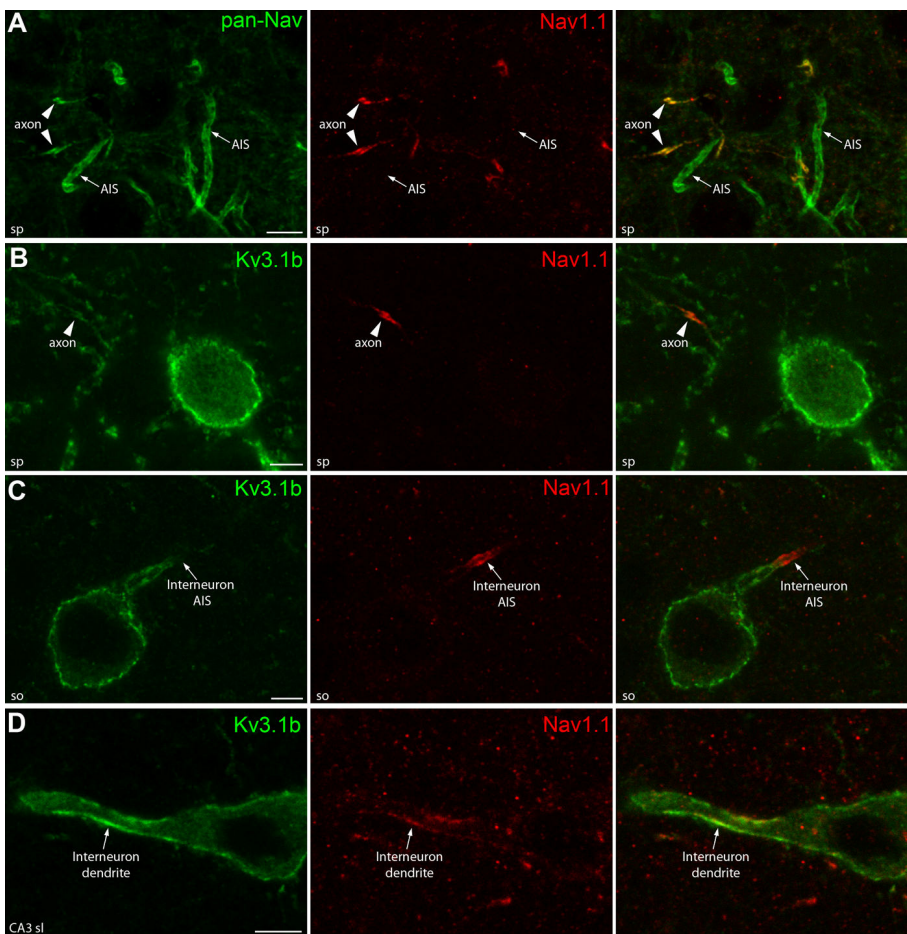


**Fig. S3.** Immunofluorescence localization of the Nav1.1 subunit in hippocampal interneurons. **(A)** Immunolabeling for the Nav1.1 subunit (red) is present in pan-Nav labeled (green) small profiles (arrowheads) in the stratum pyramidale of the CA1 area. No immunoreactivity for the Nav1.1 subunit could be detected in the AIS of PCs (arrows), which were strongly immunolabeled with the pan-Nav antibody. **(B)** Double immunofluorescence reaction in the stratum pyramidale of CA1 area reveals the presence of the Nav1.1 subunit (red) in small axons (arrowhead) of interneurons immunopositive for the Kv3.1b subunit (green). **(C)** Double immunofluorescence reaction in the stratum oriens shows intense immunolabeling for the Nav1.1 subunit (red) in the AIS of an interneuron identified by Kv3.1b subunit immunolabeling (green). **(D)** Immunolabeling for the Nav1.1 subunit (red) is found in the proximal dendrite of a Kv3.1b subunit immunopositive (green) interneuron in the CA3 stratum lucidum (sl). Scale bars: 5 $\mu$ m.

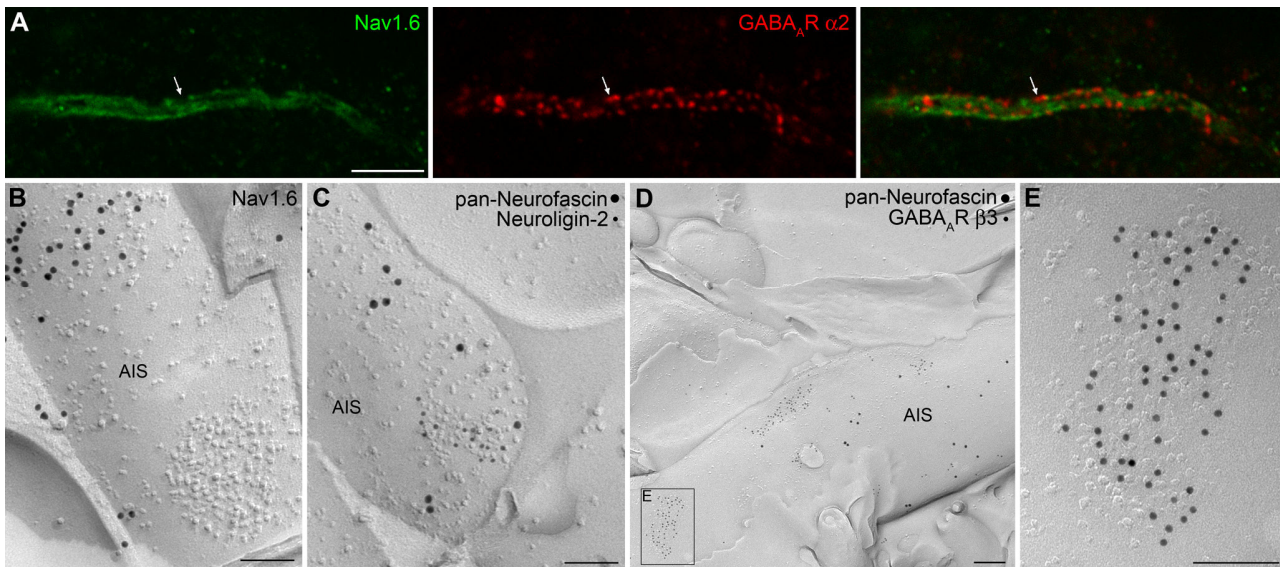


**Fig. S4.** Axo-axonic GABAergic synapses devoid of Nav1.6 subunit labeling. **(A)** Double immunofluorescent reaction in the stratum pyramidale of the CA1 area shows an AIS immunopositive for the Nav1.6 subunit (green) and covered by numerous synaptic puncta labeled by the GABA<sub>A</sub> receptor  $\alpha$ 2 subunit (red). The Nav1.6 subunit immunolabeling does not co-localize with the synaptic receptors (arrow). **(B)** High magnification image of the AIS shown in Fig. 3A. Gold particles labeling the Nav1.6 subunit are excluded from the IMP cluster and its immediate vicinity. **(C)** 10 nm immunogold particles labeling Neuroigin-2 accumulate over an IMP cluster on the P-face of an AIS identified by pan-Neurofascin labeling (15nm gold particles) in the CA1 area. **(D)** Distribution of GABA<sub>A</sub>R  $\beta$ 3 subunit immunolabeling (10nm gold particles) on the P-face of an AIS identified by pan-Neurofascin labeling (15nm gold particles). **(E)** High magnification image of the boxed area in D reveals the accumulation of 10 nm gold particles labeling the GABA<sub>A</sub>R  $\beta$ 3 subunit over the IMP cluster. Scale bars: **A**, 5  $\mu$ m; **B**, **C**, **E**, 100 nm; **D**, 200 nm.



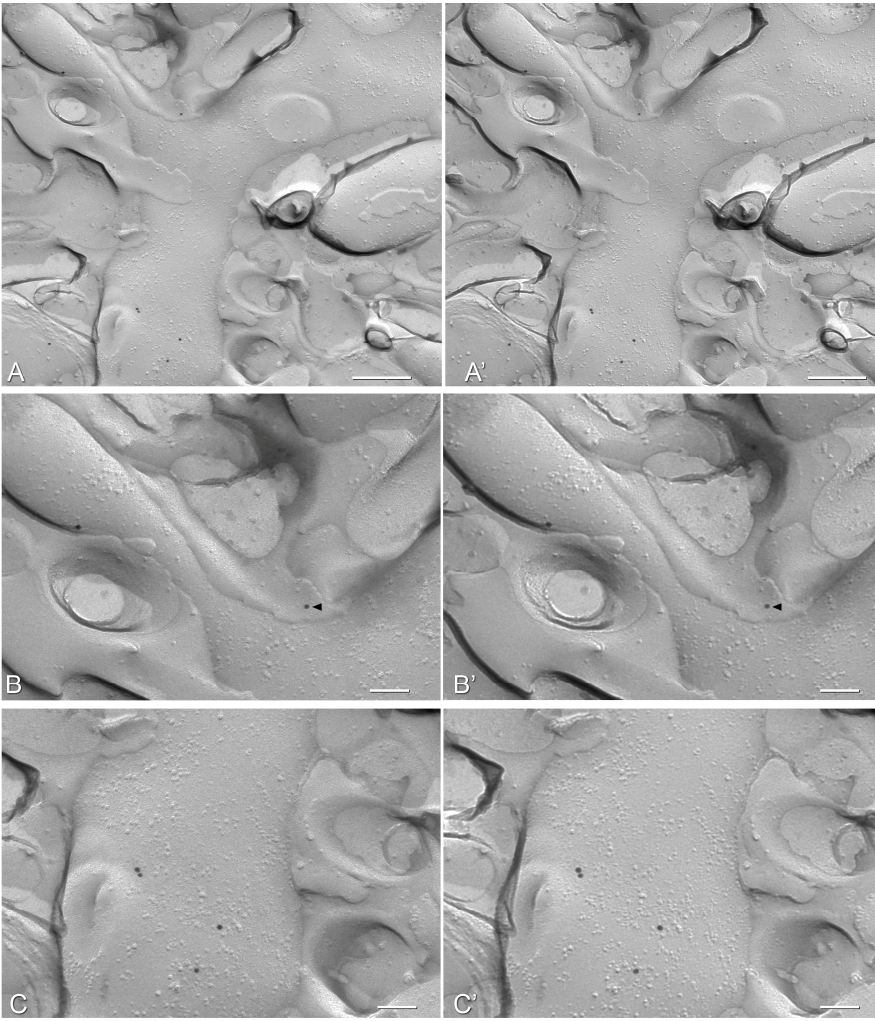


**Fig. S5.** Stereoscopic pairs of electron microscopic images taken from the stratum radiatum of the CA1 area show SDS-FRL immunogold reaction for the Nav1.6 subunit. **(A)** A dendritic spine emerges from an immunopositive small diameter oblique dendrite. The dendrite and the spine are fractured to the P-face. **(B)** Higher magnification view of the spine and the surrounding area. A presumed glial process just adjacent to the spine is fractured to E-face and contains a single gold particle (arrowhead). Stereo viewing the images demonstrates that this particle is present on the top side of the replica. **(C)** Higher magnification view of the dendritic shafts containing four gold particles. Stereo investigation reveals that all four particles are below the replica. Scale bars: **A**, 200 nm; **B**, **C**, 100 nm